DETECTION OF WEAK LASER PULSES BY FULL WAVEFORM STACKING

U.Stilla [a], W. Yao [a, *], B. Jutzi [b]

[a] Photogrammetry and Remote Sensing, Technische Universitaet Muenchen, Arcisstr. 21, 80290 Munich, Germany
(uwe.stilla, wei.yao)@bv.tum.de
[b] Research Institute for Optronics and Pattern Recognition, FGAN-FOM, 76275 Ettlingen, Germany
jutzi@fom.fgan.de

KEY WORDS: Weak pulse signal, Pulse detection, Waveform, Stacking, Laser scanning, Correlation.

ABSTRACT:

Pulse detection is a fundamental task of processing data of pulsed laser systems for extracting features of the illuminated object. Weak pulses below the threshold are discarded by classic methods and the involved information will get lost. In this paper we present an approach for detecting weak pulses from waveform laser data based on analyzing neighbourhood relations given by coplanarity constraint. Waveform stacking technique is used to improve the signal to noise ratio (SNR) of object with poor surface response by means of mutual information accumulation, thus hypotheses for planes of different slopes are generated and verified. Each signal is assessed by a likelihood value with respect to accepted hypotheses. At last signals will be classified according to likelihood values using two thresholds and visualized by the traffic-light paradigm. The presented method was applied as a low-level operation to a whole waveform cuboid of an urban area and shows promising results. Results contain detected pulses reflected from objects, which can not be predicted by the previously detected point cloud.

1. INTRODUCTION

Nowadays commercial full-waveform laser scanning systems are available to capture the waveform of the backscattered laser pulse. Beside the large-footprint spaceborne system, namely Geoscience Laser Altimeter System (GLAS) (Brenner *et al.*, 2003), additional small-footprint airborne systems are available: the Scanning Hydrographic Operational Airborne Lidar Survey system (SHOALS) is used for monitoring nearshore bathymetric environments (Irish & Lillycrop, 1999), where the OPTECH ALTM 3100, TOPEYE MK II, and TOPOSYS HARRIER 56 (it contains the RIEGL LMS-Q560) are mainly used to survey forestry environment (Hug *et al.*, 2004; Reitberger *et al.*, 2006; Söderman *et al.*, 2005).

Typically for these systems the waveform is captured for a predefined range interval, where the backscattered laser pulses are expected or a trigger signal is detected. Then the measurement of a scene containing objects expanded over a large range area may lead to an incomplete recording, because the range area is above the predefined range interval. For our investigations we use data of an experimental laser scanning system that allows capturing the complete full-waveform data within a range area of 200m.

The recording of the received waveform offers the possibility for the end user to select different methods to extract features and range information. The most popular methods are peak detection, leading edge detection, average time value detection, and constant fraction detection. This topic was investigated by different authors, e.g. Der *et al.*, 1997; Jutzi & Stilla, 2003; Wagner *et al.*, 2004. To derive a parametric description of the pulse properties range, width and amplitude a decomposition method on the waveform is proposed by Hofton *et al.* (2000). Further improvements on reliability and accuracy can be derived by signal processing methods based on the transmitted and the received waveform, e.g. cross-correlation (Hofton & Blair, 2002) and inverse filtering (Jutzi & Stilla, 2006).

When a threshold-based approach is used, attenuation of the signal by transmission through aerosol, fog, rain, snow, etc., reflection on a weakly backscattering cross section, or strong material absorption can produce subliminal signal values, where the detection of the object is not possible. Full-waveform laser data has provided us a possibility to utilize the neighborhood relation between laser signals, which can be utilized to support pulse detection. This idea is based on the common characteristic of man-made objects in the scene – regular distribution in local neighbourhood.

In this work we investigate full-waveform data with weak laser pulses by exploiting neighbourhood relation to support pulse detection. The experimental setup for a fast recording of a scene with different urban objects is described in section 2. Section 3 gives us a detailed description and discussion of purposed algorithm. Results of performed test are presented in section 4.

2. EXPERIMENTAL SETUP

2.1 Laser system

The laser scanning system has three main components: an emitter unit, a receiver unit, and a scanning unit.

For the emitter unit, we use a short duration laser pulse system with a high repetition rate (42 kHz). The pulsed Erbium fibre laser operates at a wavelength of 1.55 µm. The average power of the laser is up to 10 kW and the pulse duration is 5 ns. The beam divergence of the laser beam is approximately 1 mrad.
The receiver unit to capture the waveform is based on an optical-to-electrical converter. This converter contains an InGaAs photodiode sensitive to wavelengths of 900 to 1700 nm.

* Corresponding author.

Furthermore, we use a preamplifier with a bandwidth of 250 MHz and an A/D converter with 20 GSamples/s.

The scanning unit for the equidistant 2-d scanning consists of a moving mirror for elevation scan (320 raster steps of 0.1°) and a moving platform for azimuth scan (600 raster steps of 0.1°). The field of view is 32° in vertical and 60° in horizontal direction.

2.2 Test scene

For the investigations, a measuring platform is placed at a height of 15 m, pointing at an outdoor scene. The different urban objects in the scene are buildings, streets, vehicles, parking spaces, trees, bushes, and grass. Some objects are partly occluded and the materials show various backscattering characteristics.

2.3 Scanning and data

For each orientation of the beam within the scanning pattern, the emitted signal and the received signal are recorded over the time t for the time interval $t=t_{min}$ to $t=t_{max}$. The time interval selected for the recording of the signal depends on the desired recording depth of the area (in our case up to 200m). For each discrete range value the intensity value of the pulse is stored. The entire recording of a scene can be interpreted and visualised as a discrete data cuboid I[x y t], where the measured intensity at each time t and each beam direction [x y] is stored. It has to be taken into account the recording geometry for correct interpretation of the data.

3. STRATEGY

An automatic approach for detecting laser weak pulses based on neighbourhood relation preserved in the waveform cuboid is presented in this section.

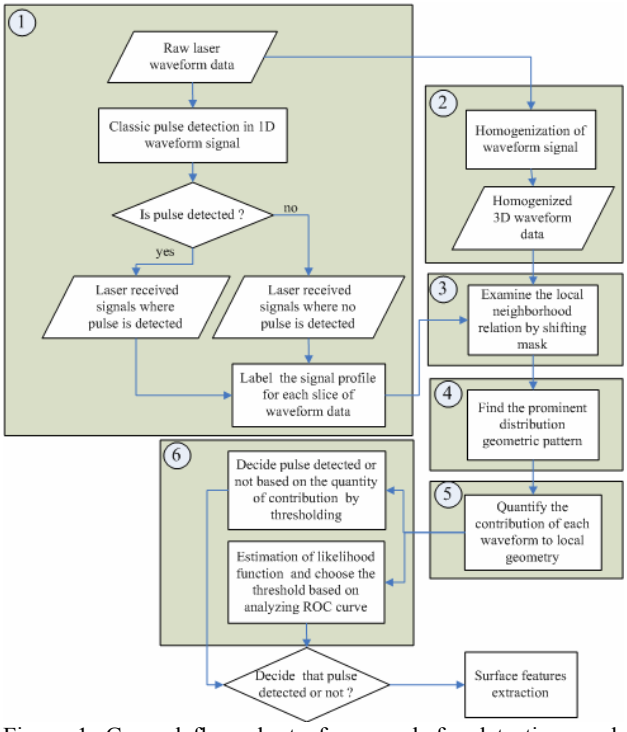

Figure 1. General flow chart of approach for detecting weak signal

The general strategy is sketched in Fig. 1. At first, a classic pulse detection method is adopted to extract the significant pulse signal backscattered from objects. Every laser ray in the waveform cuboid will be labelled as detected or undetected. On the other hand, the waveform cuboid is undergone a homogenization process. Afterwards, we generate a 1-D mask and shift it through every vertical slice of waveform cuboid to analyze the local neighbourhood relation by waveform stacking, and the prominent geometric pattern can be found. By comparing original waveforms to averaged stacked waveform the contribution of each waveform to local geometry can be assessed by a likelihood value. At last, according to this value, we can attribute a class (***'pulse', 'no pulse' or 'uncertain'***) to every original waveform by selecting thresholds in advance or by statistical inference.

3.1 Classic pulse detection method

Because of algorithmic efficiency and simplicity, it is always wise to apply the classical 1-D pulse detection methods (e.g. peak detection or correlation method) to raw waveform data firstly; high-energy reflected pulse can be detected, as displayed in Fig. 2. The rest laser rays where no pulse has been detected contain either weak reflection pulse from specific objects (e.g. window glass or roof behind the trees) or no backscattered signal at all due to inexistence of objects (sky)

Figure 2. Pulses detected by peak method, white pixels indicate detected pulses.

For pulse detection a noise dependent threshold was estimated to separate a signal pulse from background noise. Therefore the background noise was estimated and if the intensity of the waveform is above $3\,\sigma_n$ of the noise standard deviation for the duration of at least 5ns, then the waveform will be accepted.

For peak detection method, the range value of the detected pulses is determined by the maximum pulse amplitude, where the largest reflectance is expected. Another two typical surface features are roughness and reflectance which correspond to width and amplitude of waveform. Then, a Gaussian curve can be fitted to recorded waveform to get a parametric description using iterative Gauss-Newton method ((Jutzi & Stilla, 2006)). The estimated parameters for waveform features are the average time τ , standard deviation σ and maximum amplitude a .

$$w(t) = \frac{a}{\sqrt{2\pi\sigma^2}} \exp\left(-\frac{(t-\tau)^2}{2\sigma^2}\right) \qquad (1)$$

According to results of the classic pulse method, every waveform of laser beams will be labelled as detected (1) or undetected (0) and arranged in arrays corresponding to various vertical slices for further study.

3.2 Homogenization of waveform laser data

As stated above the raw waveform signal recorded by an experimental laser system is noisy and has strong fluctuation caused by the emitted pulse. In Fig. 3a, a section of waveform is plotted overlaid with an adjacent waveform reflected from surface of same material. The none-pulse part (indicated by two arrows in Fig.3a) of blue waveform shows a lower amplitude value than the corresponding part of red one, actually, they should be recorded in same level.

The waveform data cuboid should provide us a unified and consistent data base; otherwise it is difficult to exploit neighbourhood relations hiding in it. Therefore a pre-processing step needs to be performed to normalize the whole data set. The y-t slice of the cuboid is expected to exhibit more consistent after homogenization, when observed from side-look.

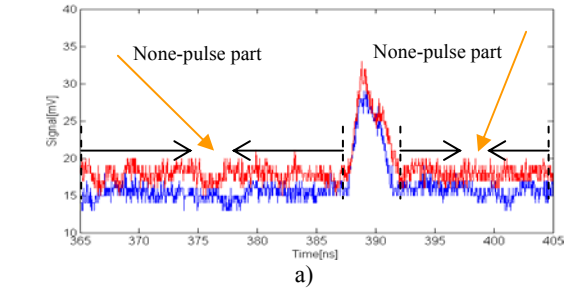

Figure 3. Necessity of homogenization operation a) neighbouring raw waveforms, b) e-t (elevation-temporal) slice image section before homogenization, c) after homogenization.

The homogenized waveform data is generated via the zero-mean operation, namely every waveform along the travel path of laser will be built into a zero-mean signal by subtracting its own mean value, and thus the waveform amplitude inside a slice or among the different slices will become consistent. The strip noise that was obvious previously (Fig. 3b) has decreased. (Fig. 3c)

3.3 Examine neighbourhood relation

Test scene was scanned by an experimental laser sensor in the order of e-r slice (elevation angle – range); the recorded waveform cuboid was also organized in the structure of e-t slice image, therefore we decided to utilize the local neighbourhood relation in this 2D image, namely to examine whether there are pulses hiding in waveforms of the local neighbourhood tending to demonstrate an identical geometry and enhance each other by mutual information, e.g. lying in an regular geometric pattern, in our algorithm this geometric pattern is limited to plane, namely straight line in 2D waveform slice.

We create a $1 \times 14 \times t$ (14 pixels in E axis is a little larger than minimum size of plane we assume; t is equal to number of range values of waveform) mask and shift it inside a slice along elevation angle direction (Fig.4 b), the step size of mask shift is half of mask size in y axis to guarantee 50% overlapping. By shifting this mask, we can process all the recorded waveforms successively without any prior information given beforehand.

While shifting the mask along the y axis, it is obvious that we have to distinguish between two different situations for considering the local neighbourhood relation – waveforms of detected pulse and those of undetected pulse.

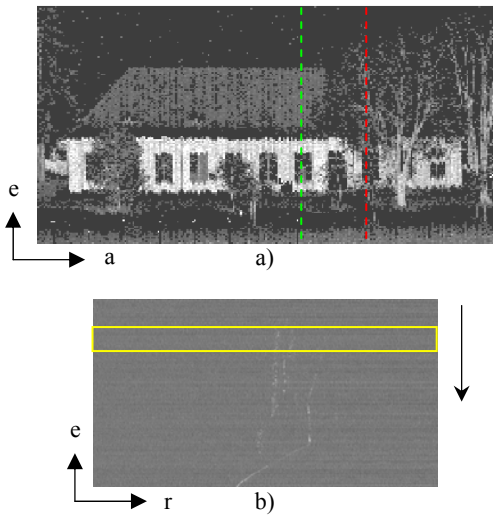

Figure 4. Mask shifting operation a) amplitude image generated by peak detection (e-a view, black pixels indicate waveforms of undetected pulse), b) e-r slice image marked by red dotted line, yellow rectangle denotes the mask, the black arrow denotes shift direction

3.3.1 Waveform of detected pulse

For the waveforms where pulse is already detected, its features, such as range, width and amplitude, are available by fitting Gaussian curve into pulse signals simultaneously. We can use the coordinate information of scattered points, which is represented in the vector format, to yield the local neighbourhood relation directly.

Principal component analysis (PCA) has been chosen here to accomplish this task. We regard three coordinates [x y t] as observed variable $\mathbf{x}$, and fit an n-dimensional hyperplane in 3-dimensional space ($n < 3$). The choice of r is equivalent to choosing the number of components to retain in PCA. When we want to evaluate whether the detected pulses are located in a straight line to build a local geometric pattern and how good they do, the variance of each component can act as the measure for it, because each component explains as much of the variance in the data as is possible with the relevant dimension.

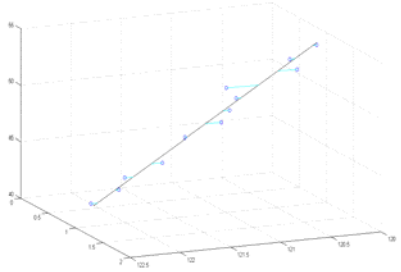

Figure 5. Local neighbourhood relation (line) found for detected pulses (blue circle) via PCA

The latent roots (or eigenvalues of covariance matrix $\mathbf{C}$) from the PCA define the amount of explained variance for each component, and the proportion of each variance can be derived:

$$\mathbf{C} = \mathbf{E}[\mathbf{B} \otimes \mathbf{B}] = \frac{1}{N}\mathbf{B} \cdot \mathbf{B}^*$$

$$\mathbf{V}^{-1}\mathbf{C}\mathbf{V} = \mathbf{D} \qquad (2)$$

where $\mathbf{B}$ is mean-subtracted matrix of $\mathbf{x}$, $\mathbf{D}$ is the diagonal matrix of eigenvalues of $\mathbf{C}$, $\mathbf{V}$ is matrix of eigenvectors diagonalizing the covariance matrix $\mathbf{C}$.

$$\begin{aligned} \text{roots} &= \mathbf{diagonal}(\mathbf{D}) \\ \text{propoVAR} &= \text{roots/sum(roots)} \\ &= [0.998 \quad 0.001 \quad 0] \end{aligned} \qquad (3)$$

As showed above the variance of first component has held a dominant proportion against other components according to propoVAR, the straight line is the best 1-D linear approximation to the data (Fig 5).

3.3.2 Waveform of undetected pulse

For another group of waveforms where pulse is not detected yet, we must deal with whole waveform signal instead of point cloud. Waveform stacking method is adopted to locate potential geometric pattern within the mask.

Image stacking technique is used to increase the signal to noise ratio (SNR) of weak objects in the final output image. This basic idea can be easily transformed to the concept of waveform stacking. We take the 1D signal along laser ray as the unit for waveform stacking, and try to identify prominent peak information in the stacked waveforms generated along specific slopes, which means existence of significant regular geometry such as plane. By stacking multiple waveforms on top of each other along different slopes, the weak pulse is expected to be enhanced against the random noise. The random noise will be counteracted with each other in spite of low SNR, whereas the true reflection information representing object features will be emphasised to some level, so they can be identified again.

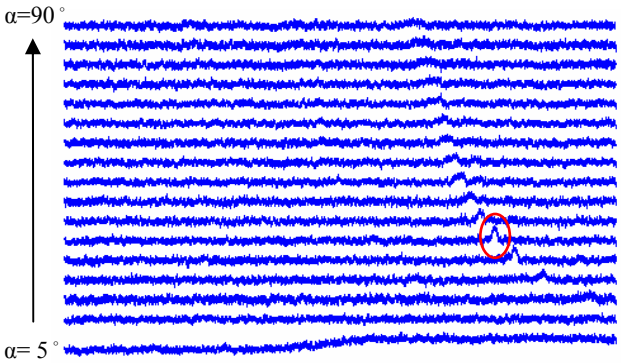

Figure 6. Waveform stacking along slope angles from $\alpha = 5^\circ$ to 90°, in steps of $\Delta\alpha = 5^\circ$ for roof area (from the slice marked by green dotted line in Fig 4a). Red ellipse marks the maximal peak information of the best stacked waveform.

Through waveform stacking, we can obtain a series of stacked waveforms corresponding to various stacking slope angles (Fig.6). When there is only one significant distribution of regular geometry like straight line, only one maximal peak signal interval of certain stacking slope angle corresponding to local geometry can be identified, and the result of waveform stacking along this slope is called best stacked waveform. If there are barely or multiple distinct peak signals, we fail to find out the regular geometric pattern in local neighbourhood due to no or ambiguity of extremum distribution, such as sky and holes and volume scatters (tree leaves).

In Fig 7 the cyan curve denotes the maximal value of stacked waveform along each slope toward stacking angle. The red curve is the smoothed version of the cyan curve. The approximation of red curve by cubic is plotted in magenta. Thus, the slope angle of best stacked waveform can be improved by locating maximum of fitting curve with "sub-pixel" accuracy. The green dotted line indicates the max value of cubic.

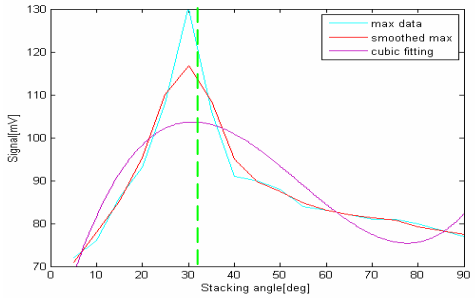

Figure 7. Maximum values of stacked waveforms vs. stacking slope angle

3.4 Find the prominent geometric pattern

After examining the local neighborhood relation for waveforms of detected and undetected pulses respectively, we have to consider them as an entirety. The local neighbourhood where both kinds of pulses coexist is examined by shifting a mask (Fig.8a). The prominent geometric pattern for a mixed set of waveforms (detected and undetected pulses) within the mask has to be identified and is to be recorded in a data list $\{\mathbf{P}_i\}$.

First we have to distinguish between three different situations encountered while shifting the mask (Fig.8b):

a) Waveform of undetected pulse almost occupies the mask, Number (Num) of $\{\mathbf{waveform\ of\ no\ pulse}\} > 9$

b) Waveform of detected pulse almost occupies the mask
Num of $\{\mathbf{waveform\ of\ pulse}\} > 9$

c) Both kinds of waveforms appear balanced
Num $\{\mathbf{waveform\ of\ pulse}\} < 9$ &Num $\{\mathbf{waveform\ of\ no\ pulse}\} < 9$

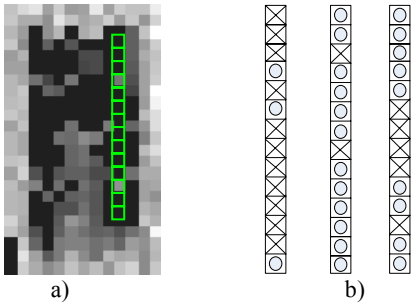

Figure 8. a) Example of mask shifted over waveform cuboid (x-y view), b) three typical situations encountered, circle indicates waveform of pulse detected, and cross indicates waveform of no pulse

Algorithm Find out prominent geometric pattern from the waveforms delimited by mask

Input: Waveform slice, label array by point cloud
Initialize Prominent geometric pattern list $\{\mathbf{P}_i\}$
while $\{\mathbf{S}\}$ **is not reached**
  if Num $\{$**waveform of no pulse**$\} > 9$ **then**
    Examine geometric pattern via waveform stacking
  else if Num $\{$**waveform of pulse**$\} > 9$ **then**
    Examine geometric pattern via PCA
  else
    Examine geometric pattern for two kinds of waveform respectively, and define a multiple neighborhood relations for waveforms
  end if
  end if
  if the geometric pattern is found **then**
    Add to prominent geometric pattern list $\{\mathbf{P}_i\}$ for this local mask
  end if
end while
Return $\{\mathbf{P}_i\}$

The algorithm described above has given us prominent geometric pattern list $\{\mathbf{P}_i\}$ as result. If a multiple neighborhood relation is defined for 3rd situation, the waveforms will be treated in terms of different geometric patterns. For some local waveform groups covered by the shifting mask, there may be no prominent geometric pattern found, e.g. sky or holes, the next processing step (Fig.1-5) will be skipped and the likelihood value for assessing weak pulses is set to zero directly.

3.5 Contribution determination of single waveform

In the last step of the whole algorithm, a measure should be defined to evaluate relation between the single original waveforms and local geometric pattern found by analyzing the local neighborhood relation. This measure quantifies how the single waveform contributes to building the prominent geometric pattern and can be further perceived as the likelihood value for assigning the corresponding waveform as pulse or not.

On the basis of considerations above, the correlation coefficient ρ between both waveform sections is calculated and used to serve as the measure, which describes similarity between the shape of waveforms to be compared.

$$\rho(i,j) = \frac{\mathrm{cov}(i,j)}{\sqrt{\mathrm{var}(i,i) \times \mathrm{var}(j,j)}} \quad \textbf{and} \quad -1 \le \rho(i,j) \le 1 \qquad (3)$$

For those local neighbourhoods whose prominent geometric pattern is built by waveforms of undetected pulse, the peak signal fraction will be cropped from the averaged stacked waveform (section between two green lines in Fig.9). We compare this peak signal fraction to the corresponding section of original waveform through correlation in order to acquire the contribution of every original waveform to the best stacked waveform. The same procedure is performed towards another kind of local neighbourhood, only the averaged stacked waveform will be replaced by averaged waveform of detected pulse. As a result of existence of overlapping areas through shifting the mask and multiple neighborhood relations, the identical waveform may be repeated to correlate with multiple prominent geometric patterns, from which the maximal correlation coefficient will be chosen as the likelihood value for this waveform.

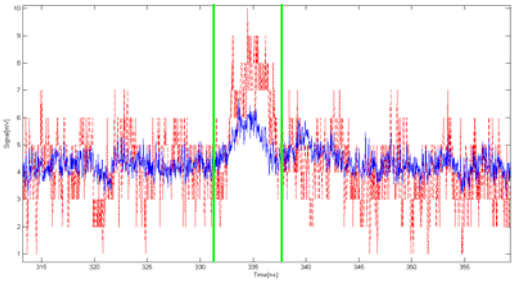

Figure 9. Original waveform (red) plotted overlaid with averaged stacked waveform corresponding to the prominent geometric pattern.

The hypothesis of weak pulses to be detected or not can be verified based on the likelihood value. This is the problem of two-class classification; one has to make a decision between two hypotheses either by thresholding empirically or based on estimation of likelihood function.

4. RESULTS

The presented algorithm was applied to the waveform data cuboid acquired by an experimental laser system. According to the correlation coefficient, detection of weak pulses can be achieved by two-class classification. For those experiments, where we do not have any priori-knowledge or assumption concerning pulses expected to be detected, we decide pulse detected or not by selecting threshold empirically. In order to make the detection results more flexible and avoid crisp decision, up (t_u) and bottom (t_b) thresholds are to be set, if $\rho(waveform) \le t_b$ then accepted as detected pulse, if $\rho(waveform) \ge t_u$ then fail to detect pulse, if $t_b < \rho(waveform) < t_u$ remain to be checked further, and so we used a traffic-light paradigm to visualize the detection result which is shown in Fig 10. The most signals lying among roof region (without occlusion) are classified as detected pulse requiring no further check, whereas the most ones in the sky belong to the red category rejected directly(Fig.10). This result corresponds to our expectation and demonstrates reasonability of the algorithm.

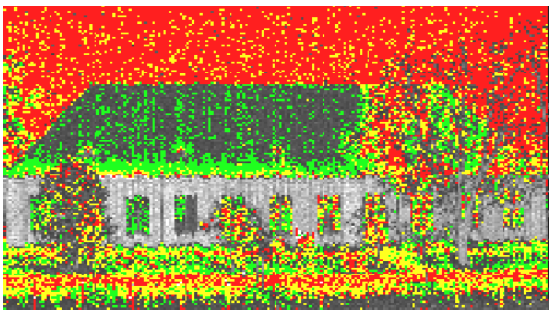

Figure 10. Result of weak pulse detection (x-y view), Red: no pulse; Yellow: uncertain; Green: pulse

For two critical parts of the test scene – window and roof behind trees, a number of signals have been detected, thus the object feature can also be recovered (Fig.11a, b), e.g. the detected weak signals almost lie in one plane, moreover, the window plane formed by detected pulses appears to lie in some offsets backwards with respect to wall; The outline of the roof partially occluded by tree is to certain degree recovered. Many signals reflected from the ground have failed to be detected

perhaps due to poor local neighbourhood relation and very weak reflection.

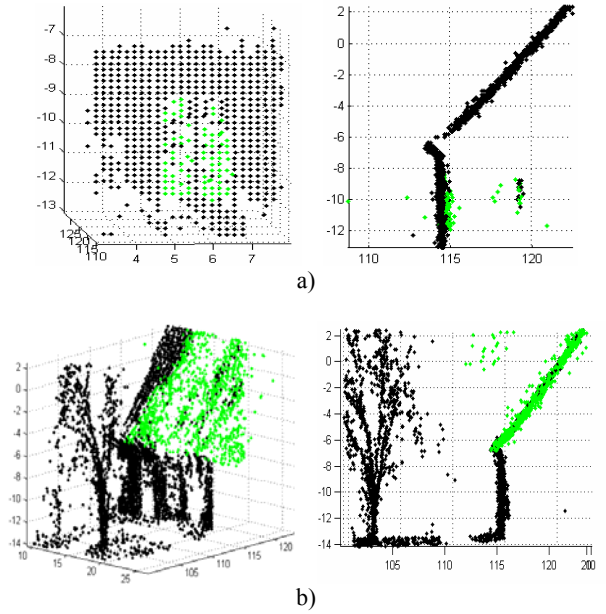

Figure 11. Results of local sections of test scene a) point cloud of window section with detected weak pulses showed in green from front and side view, b) section of roof behind the tree

After making a decision on three categories, the yellow category will be delivered to a further check based on SNR, so that we can finally obtain a result of only two classes - detected or not detected. In Fig.12 the relative histograms of correlation coefficient of two classes are depicted overlaid with each other. The Gaussian curve used to fit to the histograms can be perceived as an approximation of likelihood function for each hypothesis, few overlapping area proved separability of two classes and appropriateness of correlation coefficient as feature value.

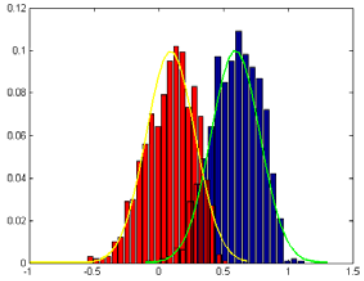

Figure 12 Overlapping relative histograms of correlation coefficients of two classes – pulse detected (blue) and not detected (red), with corresponding Gaussian fitting.

5. CONCLUSION

In this work an automatic approach for extracting weak laser pulses from full-waveform laser data has been presented. The algorithm uses waveform stacking to analyze the local neighbourhood of laser signals. Hypotheses for planes of different slopes are generated and verified. Each signal is assessed by a likelihood values with respect to accepted hypotheses. This contribution measure to local geometry is used for the subsequent operation of detection. The results on waveform data acquired from urban area show ability to detect partially occluded objects or objects with poor surface response, which can not be geometrically predicted by previous detected point cloud. In this paper only the neighbourhood relation within a vertical slice was used, Future work will focus on hypothesis generation combining neighbouring vertical slices.

References

Brenner, A.C., Zwally, H.J., Bentley, C.R., Csatho, B.M., Harding, D.J., Hofton, M.A.,Minster, J.B., Roberts, L.A., Saba, J.L., Thomas, R.H., Yi, Y., 2003. Geoscience Laser Altimeter System (GLAS) —derivation of range and range distributions from laser pulse waveform analysis for surface elevations, roughness, slope, and vegetation heights. AlgorithmTheoretical Basis Document—Version 4.1. http://www.csr.utexas.edu/glas/-pdf/Atbd_20031224.pdf (Accessed March 1, 2007).

Der, S., Redman, B., Chellappa, R., 1997. Simulation of error in optical radar measurements. Applied Optics 36 (27), pp. 6869-6874.

Hofton, M.A., Blair, J.B., 2002. Laser altimeter return pulse correlation: A method for detecting surface topographic change. Journal of Geodynamics special issue on laser altimetry 34, pp. 491-502.

Hofton, M.A., Minster, J.B., Blair, J.B., 2000. Decomposition of laser altimeter waveforms. IEEE Transactions on Geoscience and Remote Sensing 38 (4), pp. 1989–1996.

Hug, C., Ullrich, A., Grimm, A., 2004. LITEMAPPER-5600 - a waveform digitising lidar terrain and vegetation mapping system. International Archives of Photogrammetry, Remote Sensing and Spatial Information Sciences 36 (Part 8/W2), pp. 24–29.

Irish, J.L., Lillycrop, W.J., 1999. Scanning laser mapping of the coastal zone: the SHOALS system. ISPRS Journal of Photogrammetry & Remote Sensing 54 (2-3), pp. 123-129.

Jutzi, B., Stilla, U., 2003. Laser pulse analysis for reconstruction and classification of urban objects. In: Ebner, H., Heipke, C., Mayer, H., Pakzad, K. (Eds) Photogrammetric Image Analysis PIA'03. International Archives of Photogrammetry and Remote Sensing 34 (Part 3/W8), pp. 151-156.

Jutzi, B., Stilla, U., 2006. Range determination with waveform recording laser systems using a Wiener Filter. ISPRS Journal of Photogrammetry and Remote Sensing 61 (2), pp. 95-107.

Reitberger, J., Krzystek, P., Heurich, M., 2006. Full-Waveform analysis of small footprint airborne laser scanning data in the Bavarian forest national park for tree species classification. In: Koukal, T., Schneider, W. (Eds) 3D Remote Sensing in Forestry, pp. 218-227.

Söderman, U., Persson, Å., Töpel, J., Ahlberg, S., 2005. On analysis and visualization of full-waveform airborne laser scanner data. Laser Radar Technology and Applications X. In: Kamerman, W. (Ed) SPIE Proceedings Vol. 5791, pp. 184-192.

Wagner, W., Ullrich, A., Melzer, T., Briese, C., Kraus, K., 2004. From single-pulse to full-waveform airborne laser scanners: Potential and practical challenges. In: Altan, M.O. (Ed) International Archives of Photogrammetry and Remote Sensing 35 (Part B3), pp. 201-206.